



Eidgenössische Technische Hochschule Zürich
Swiss Federal Institute of Technology Zurich

Development of an RF resonator for a double junction ion trap

Semester Project

Konstantin Nesterov

Wednesday 27th February, 2019

Advisors: Prof. Dr. J. Home, Chiara Decaroli

Department of Physics, ETH Zürich

Abstract

In this report I will describe the modeling, designing and testing of an RF helical resonator suitable for delivering RF signal to a double-junction ion trap in a cryogenic environment.

Contents

Contents	ii
1 Introduction	1
1.1 Why do we need resonators?	1
1.2 Context of this project	2
1.3 Kinds of resonators	3
1.3.1 Helical	3
1.3.2 RLC	4
1.3.3 Crystal	4
1.3.4 Choosing the right one	5
2 Theory	6
2.1 Helical resonator models	6
2.1.1 Macalpine & Schildknecht	6
2.1.2 Siverns et al.	7
2.2 Comparison	7
3 Design	8
3.1 On a quest to perfect parameters	8
3.1.1 First iteration	8
3.1.2 Precise fit	9
3.2 Shaping the 3D model	11
3.2.1 RF resonator	12
3.2.2 Bottom cap	13
3.2.3 Shield	14
3.2.4 Helix	15
3.2.5 Helix support	16
3.2.6 Top cap	17
3.2.7 Top cap clamp	18
3.2.8 Antenna mount	19

Contents

3.2.9	Antenna	20
4	Validation	21
5	External circuits & additional features	22
A	Mathematica code for Macalpine's model	23
B	Mathematica code for Siverns' model	26
	Bibliography	30

Chapter 1

Introduction

Quantum computing is an exciting and rapidly evolving field of modern science. One of the most promising implementations of a quantum computer is based on the ability to control and measure systems of trapped ions. Those ions are typically confined in Paul (RF) [14] traps by applying static and oscillating RF signals to the trap electrodes, which on average generate a confining electric potential.

1.1 Why do we need resonators?

One could potentially couple a radio frequency source directly to an ion's trap. However this creates the following challenges:

- noise from the source may contribute to heating of trapped ions [18],
- in order to maintain efficient cryostat cooling the amount of generated heat within it should be minimized. In order to stabilize ions in the ion trap the confining RF signal must have a reasonably high voltage amplitude. An RF resonator close to the signal consumption area allows to reduce the length of an actively heated (with accordance to the Joule–Lenz law [15]) high voltage wire,
- impedance mismatch between source and trap leads to an additional dissipation of RF power.

These issues can be avoided by placing an amplifier close to the Paul trap, which would filter the incoming signal and output it with a voltage suitable for operating the trap. There are two available options: active and passive amplifiers. The core difference between them is that active amplifiers use an additional power source to increase output power of the signal while passive amplifiers rather modify the shape of the input signal conserving the overall power — in our case the voltage amplitude gain is balanced by the current amplitude decline.

1.2. Context of this project

Active amplifiers perform better in terms of voltage gain at room temperatures. However, the aim of this project is to create a resonator used within a cryogenic environment. The properties of transistors powering active amplifiers depend heavily on a combination of densities of free electrons and holes. Lowering the temperature tends to reduce [2] these densities significantly, turning semiconductors at room temperatures into practically dielectrics.

It leaves us with passive amplifiers (resonators).

1.2 Context of this project

This semester project aims to be a part of an attempt to create a scalable quantum computing architecture by Chiara Decaroli. It provides the following benefits compared to existing solutions:

- using subtractive laser writing to manufacture wafers eliminates misalignment effects by allowing a “self assembly” of different wafers,
- double junction ion trap designed for parallel operations, Decoherence Free Subspace (DFS) ion transport across the junctions, and manipulation of long chains of ions,
- potential integrated laser delivery through optical lensed fibers eliminates the need for bulky optics and custom objectives which limit scalability.

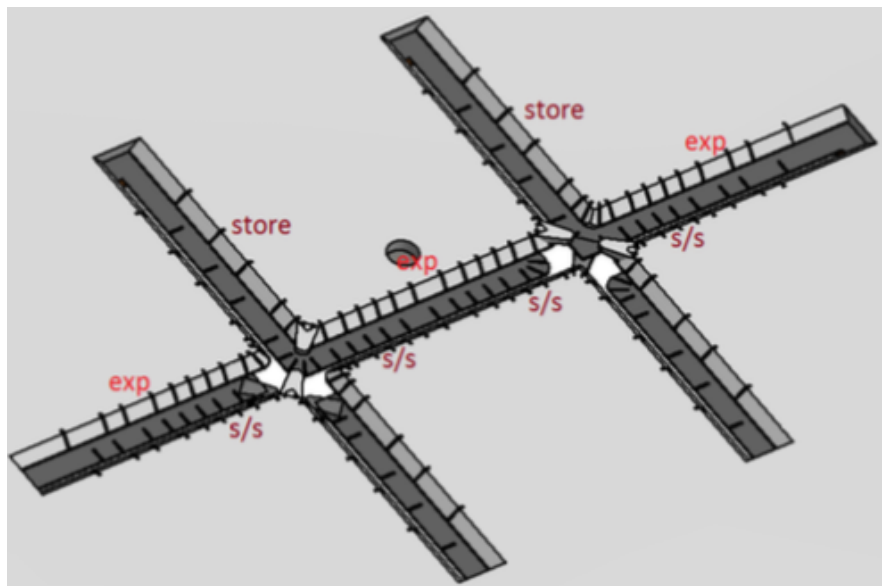


Figure 11: Ion trap overview (should be improved, just filling space now)

1.3 Kinds of resonators

The required frequency of 40 MHz limits our selection to the following types of resonators: helical [6, 7, 19, 10, 9] or, for higher frequencies, coaxial [8], RLC [4, 11, 5], and crystal oscillators. Multiple available solutions require us to do an analysis for a reasoned choice.

1.3.1 Helical

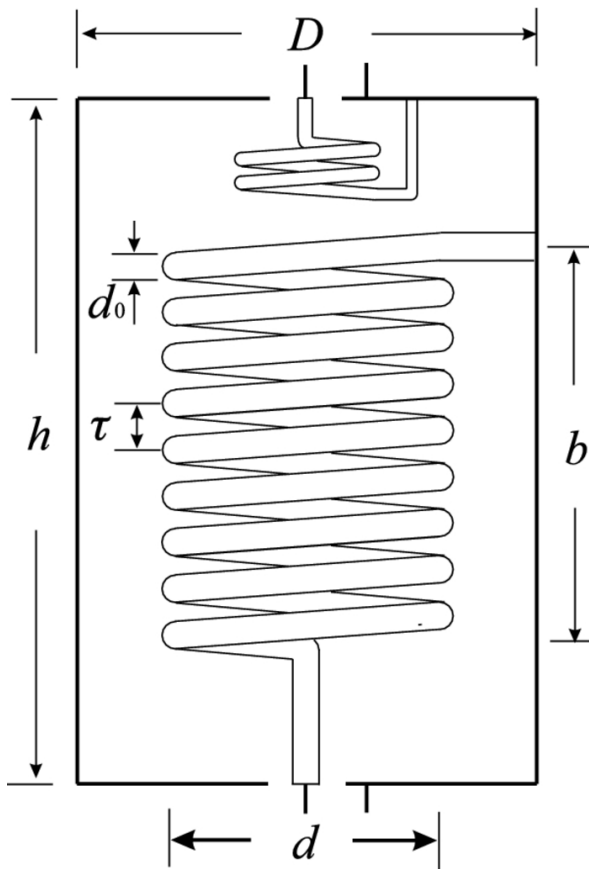


Figure 12: Schematic diagram of a helical resonator indicating shield diameter D , shield height h , coil diameter d , coil height b , winding pitch τ , and coil wire diameter d_0 . [1]

Helical resonators are commonly selected to be coupled with ion traps due to their high quality factors and ability to operate on high frequencies. It is a perfect option for ion traps operated at room temperatures, since in absence of space constraints they are able to provide Q values of a couple of thousands. However in order to achieve those Q , the fabrication process needs to be quite precise to avoid reflections of traveling waves which negatively influence the overall gain.

1.3.2 RLC

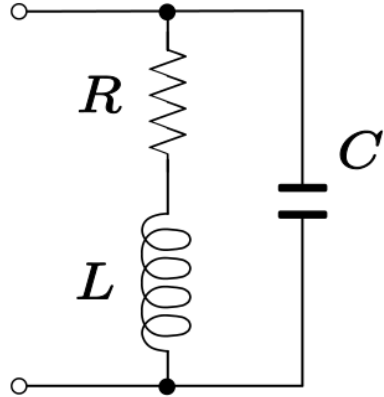


Figure 13: Example of a parallel RLC circuit

RLC amplifiers are a convenient choice for space-bounded environments, such as cryostats. Typical implementation pumps energy between two reactive components — inductor and capacitor. Assembly of RLC circuit is easier than of helical resonator since the physical placement of lumped parts does not influence the resulting quality factor. But it also means that the quality of these components is a major factor for successful creation. Given that units' data sheets rarely provide values for cryogenic setup it takes a lot of trial and error to find the right ones [4].

1.3.3 Crystal

Unlike helical and RLC resonators, the crystal oscillators do not store energy just in the electric field. This type of resonator utilizes piezoelectric effect to transform applied harmonic voltage into surface mechanical modes and vice versa.

Narrow excitation spectrum is provided by physical dimensions imposing hard constraints on vibrational oscillations and could have made such device an ideal filtering solution for ion traps. Unfortunately, there are some major downsides that seriously limit its applicability:

- after fabrication resonant frequency can not be widely tuned
- limited stability of the crystal does not allow high voltages

1.3.4 Choosing the right one

In our setup, the combination of high voltage and frequency values with our constraints on available space makes helical resonator the optimal option. However, difficulties of assembly do not make it a perfect solution in terms of scalability — for a production-grade setup RLC amplifier might be preferred.

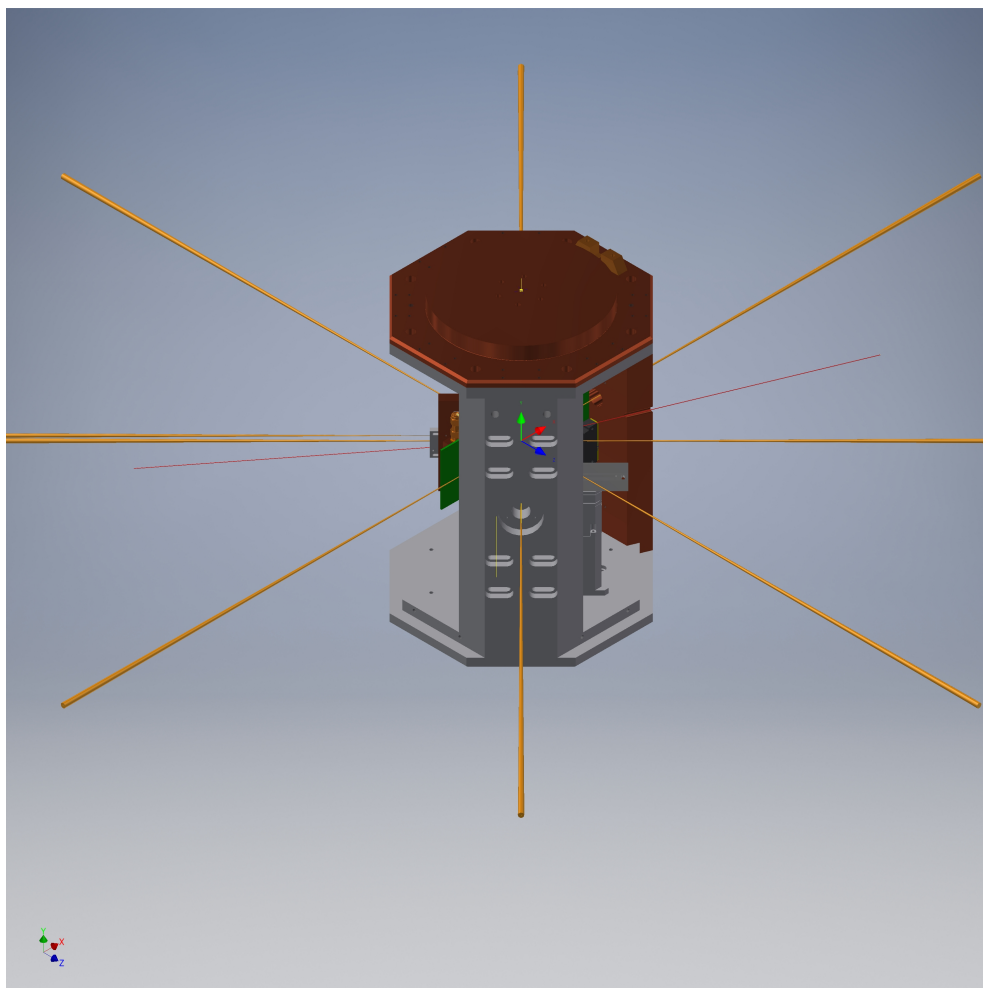


Figure 14: 3D model of the 4K cryostat chamber

Chapter 2

Theory

2.1 Helical resonator models

In order to create a helical resonator satisfying our experimental conditions and limitations we inevitably come to a need for a theoretical model that would be able to predict the essential characteristics of the resulting unit. The following sections aim to provide an overview and comparison between the models.

2.1.1 Macalpine & Schildknecht

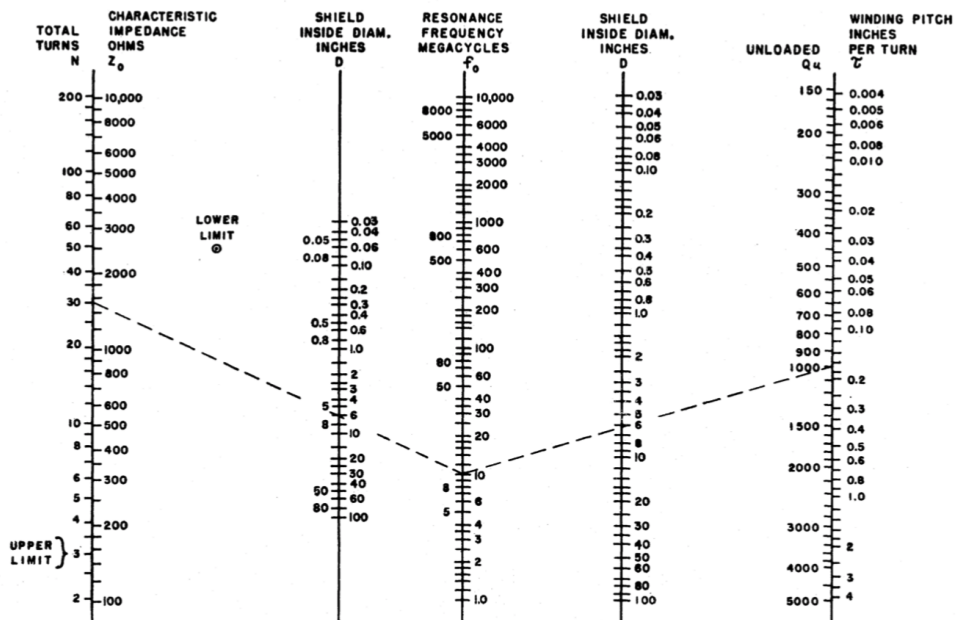


Figure 21: Design chart for quarter-wave helical resonators [13]

A well-known approach [13] for describing helical resonators was introduced in the same year as Richard Feynman's idea [3] to use quantum systems for computations. It was motivated by the possibility to reduce volume compared to TEM-mode coaxial-line resonators (90% volume reduction for the reference case [13]). While skipping a detailed theoretical analysis it nevertheless provides a basis for constructing a resonator: such as regions of usefulness, design considerations and a set of parameters' dependencies maximizing Q .

While describing essential properties of an unloaded helical quarter-wave resonator, this paper [13] also predicts the shift of resonant frequency if an external load is connected. In order to define a new frequency one can make use of telegraph equations [16] by effectively treating the ion trap as a capacitor.

Important results of [13] can be found in equations 2.1 with parameters named as in the figure 12.

$$\begin{aligned} d/D &= 0.55 \\ b/d &= 1.5 \\ h &\approx (b + D/2) \end{aligned} \tag{2.1}$$

2.1.2 Sivers et al.

Unfortunately modeling an ion trap as a pure capacitive load is not always accurate. Introducing resistive losses imposes an additional shift of resonant frequency which pushes the deviation from self-resonant frequency even further. It is possible to tune the strength of the inductive coupling between the antenna and the main coil to compensate this shift while losing in efficiency.

These limitations of Macalpine's & Schildknecht's [13] model have been overcome in a newer paper [17] which takes the development of an amplifier, specifically for the needs of quantum computing, one step further. By taking a look at the joint resonator + ion trap system as a whole it aims to predict the effective Q and frequency. This model ensures that it's possible to find optimal parameters for given experimental constraints.

2.2 Comparison

Macalpine's and Schildknecht's [13] model gives insides for designing a helical quarter-wave resonator with a given self-resonant frequency. However major shifts from it can be expected when connecting the ion trap. Sivers' et al. approach [17] investigates connections between various parameters in the total circuit. As a result one could create a resonator which implements a transfer function closer to a desired one. Considering these benefits the Sivers model [17] was selected.

Chapter 3

Design

This chapter provides a representation of efforts one must face to make a jump from dry theoretical models to a virtually real product.

3.1 On a quest to perfect parameters

Our journey begins with a necessity to define restrictions of the problem. The intended environment would be a 4K cryogenic chamber (figure 14), which imposes dimensions restrictions. The ion trap requires a defined frequency for successful confinement of ions and has a capacitance. Summarized restrictions can be found in table 31.

Parameter	Value
L_{max}	60 mm
ω_0	40 MHz
C_{trap}	10–20 pF

Table 31: Restrictions of a system

3.1.1 First iteration

Sivers' model [17] is dependent on outcomes from Macalpine's model [13] thus one needs to find these beforehand. Exact value of a trap's capacitance is unknown at the moment of calculations so it was decided to use and compare values from a following set of capacitances: $C_{trap} = [10, 15, 20]$ pF. The modified Macalpine's model, found in the appendix A, also predicts resonant frequency shift when connecting a capacitor. The unloaded frequency needed to be varied until the loaded frequency equals target frequency. Results are provided in table 32, naming is consistent with [13].

3.1. On a quest to perfect parameters

Parameter	Value		
C_{trap} , pF	10	15	20
B , mm (length of a shield)			60.0
D , mm (diameter of a shield)			45.0
b , mm (length of a coil)			37.1
N_t (number of turns)	11.0	9.2	8.1
d_0 , mm (diameter of a wire)	1.7	2.0	2.3
τ , mm (pitch of a helix)	3.4	4.0	4.6
f_0 , MHz (unloaded frequency)	97.0	116.0	132.8
Q (unloaded quality factor)	873.2	954.8	1022.4

Table 32: Joint output of the appendix A

3.1.2 Precise fit

After defining an approximate region of interest we can proceed to calculations utilizing Sivers' model [17] with implementation provided in the appendix B. Volume requirements were also better clarified with the goal to get the best quality factor by varying coil's parameters. Updated restrictions can be found in the table 33. One could argue that all values of d_0 are lower than the recommended in [17] thickness of 5 mm. This is true and additional measures to handle it can be found in section 3.2.5.

Parameter	Value		
C_{trap} , pF	10	15	20
B , mm (length of a shield)			56.0
D_{max} , mm (max diameter of a shield)			38.0
d_0 , mm (diameter of a wire)	1.7	2.0	2.3
τ , mm (pitch of a helix)	3.4	4.0	4.6

Table 33: Restrictions for the Sivers' model

Fixed values of the table 33 allow us to independently change 2 remaining parameters — diameter of a shield and diameter of a coil. Appendix's B output of Q values is provided in the figures 31, 32, 33. By selecting a point in a $\{d, \gamma = d/D\}$ space that maximizes Q for a set of C_{trap} values we get final parameters for our RF resonator as defined in the table 34.

3.1. On a quest to perfect parameters

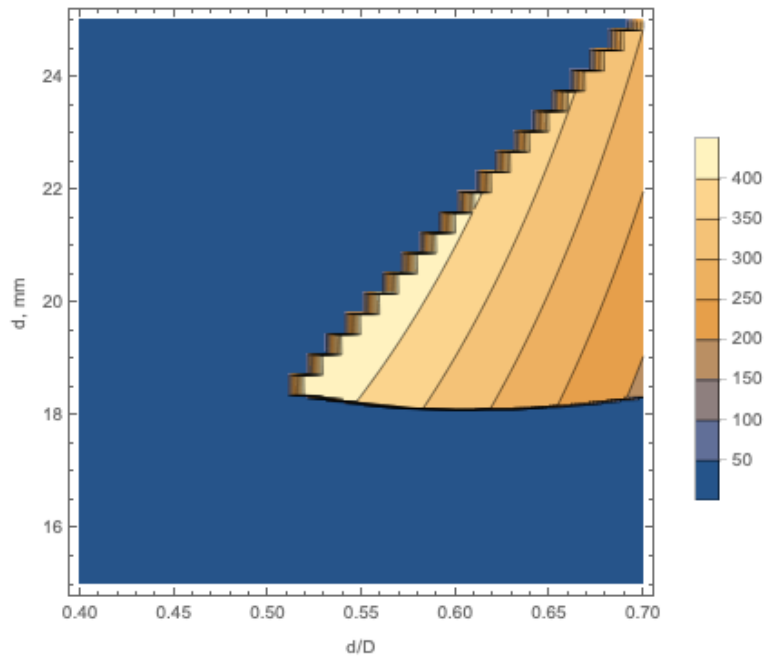


Figure 31: Q plot for $C_{trap} = 10$ pF

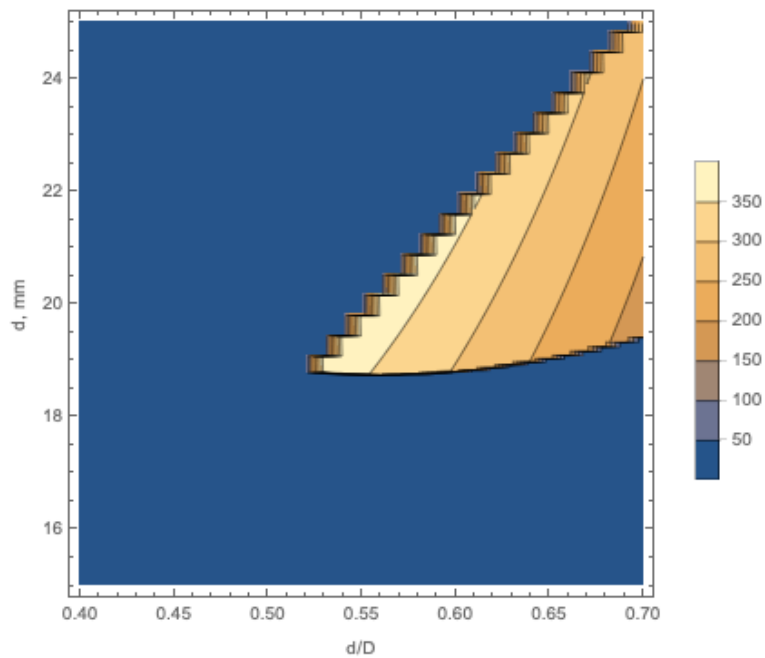


Figure 32: Q plot for $C_{trap} = 15$ pF

3.2. Shaping the 3D model

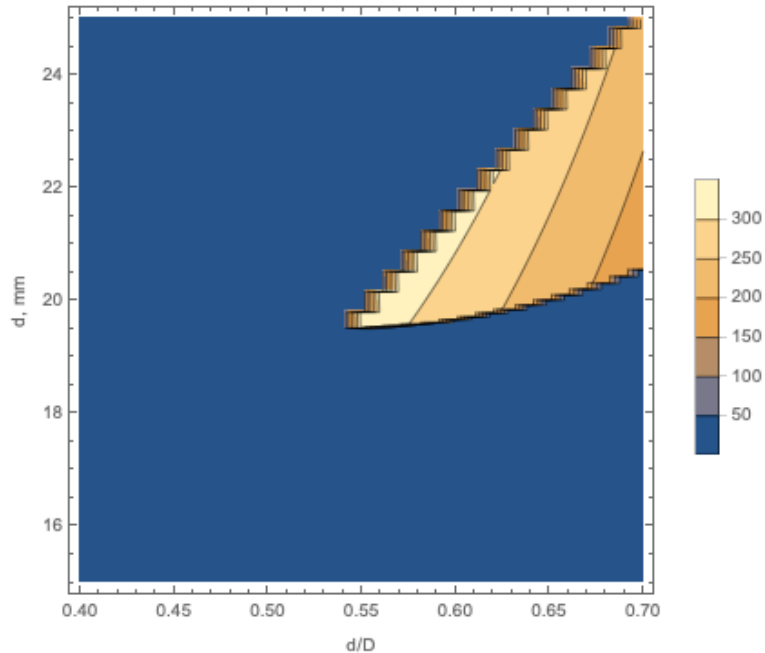


Figure 33: Q plot for $C_{trap} = 20 \text{ pF}$

Parameter	Value
B , mm (length of a shield)	56.0
D , mm (diameter of a shield)	34.5
d , mm (diameter of a coil)	19.0
b , mm (length of a coil)	40.0
N_t (number of turns)	10.0
d_0 , mm (diameter of a wire)	2.0
τ , mm (pitch of a helix)	4.0

Table 34: Final parameters of an RF resonator

3.2 Shaping the 3D model

With all dimensions in our hands we can start implementing them in a 3D design for the workshop. This section provides an overview of all parts used, their features and reasonings.

3.2. Shaping the 3D model

3.2.1 RF resonator

Assembly of the RF resonator is shown on the figure 34. Every part is produced from oxygen-free copper. Colors are adjusted for a better perception.

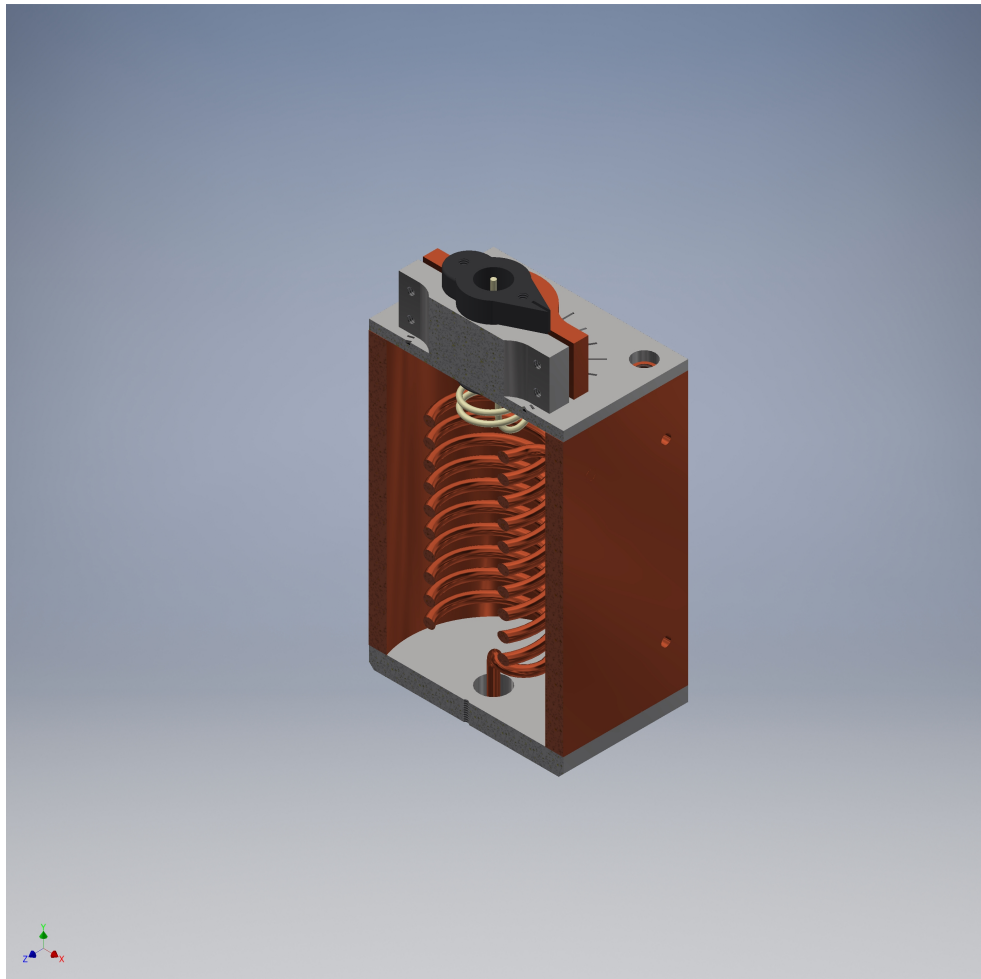


Figure 34: 3D model of an RF resonator

3.2. Shaping the 3D model

3.2.2 Bottom cap

Bottom cap as displayed in the figure 35 features:

- output hole for the helix (3.2.4)
- 4xM4 clearance holes to connect to the shield (3.2.3)
- 2xM2 thread holes for a SMA connector for the helix (3.2.4)

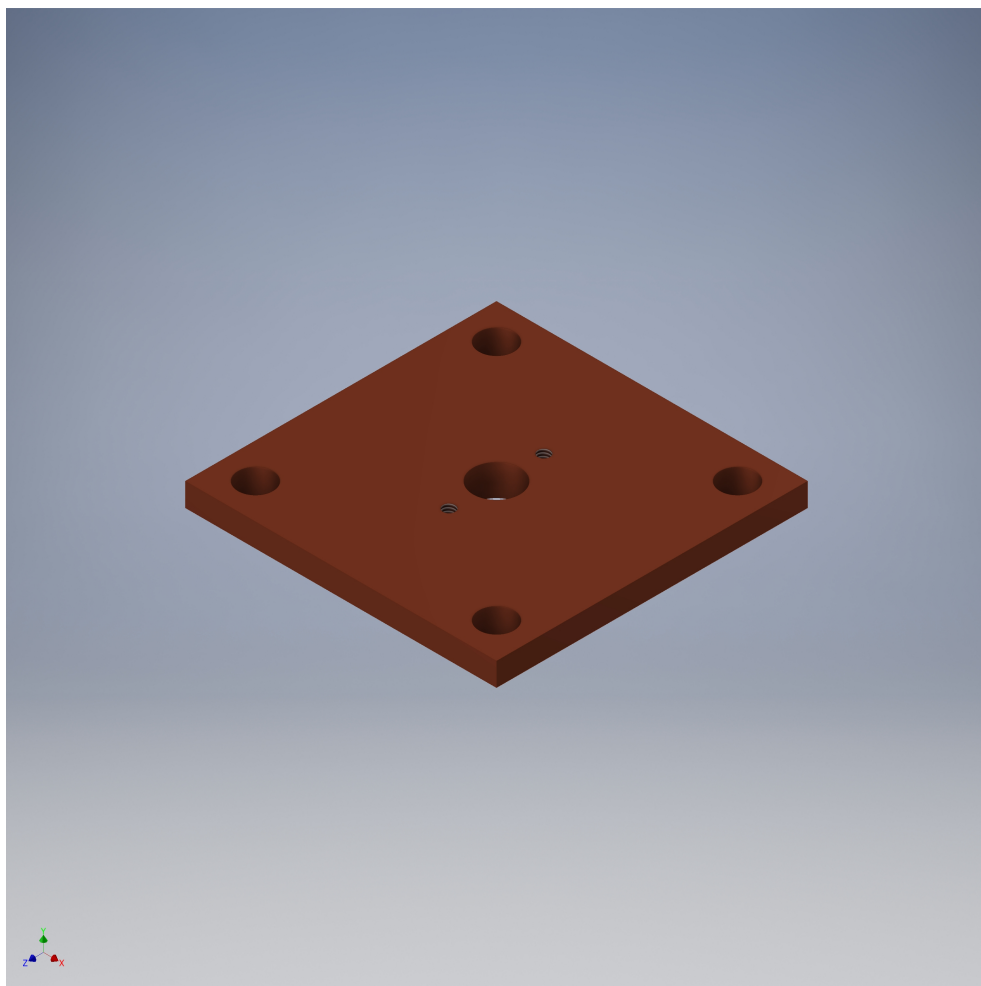


Figure 35: 3D model of a bottom cap

3.2.3 Shield

Shield as displayed in the figure 36 features:

- 4xM4 thread holes to connect to the top cap (3.2.6)
- 4xM4 thread holes to connect to the 4K chamber (figure 14)
- 4xM4 thread holes to connect to the bottom cap (3.2.2)
- 12x ventilation holes for M4 thread holes to avoid the slow leakage of the remaining air between the screw and the shield into the vacuum of the cryostat
- hole for the helix connection (3.2.4)

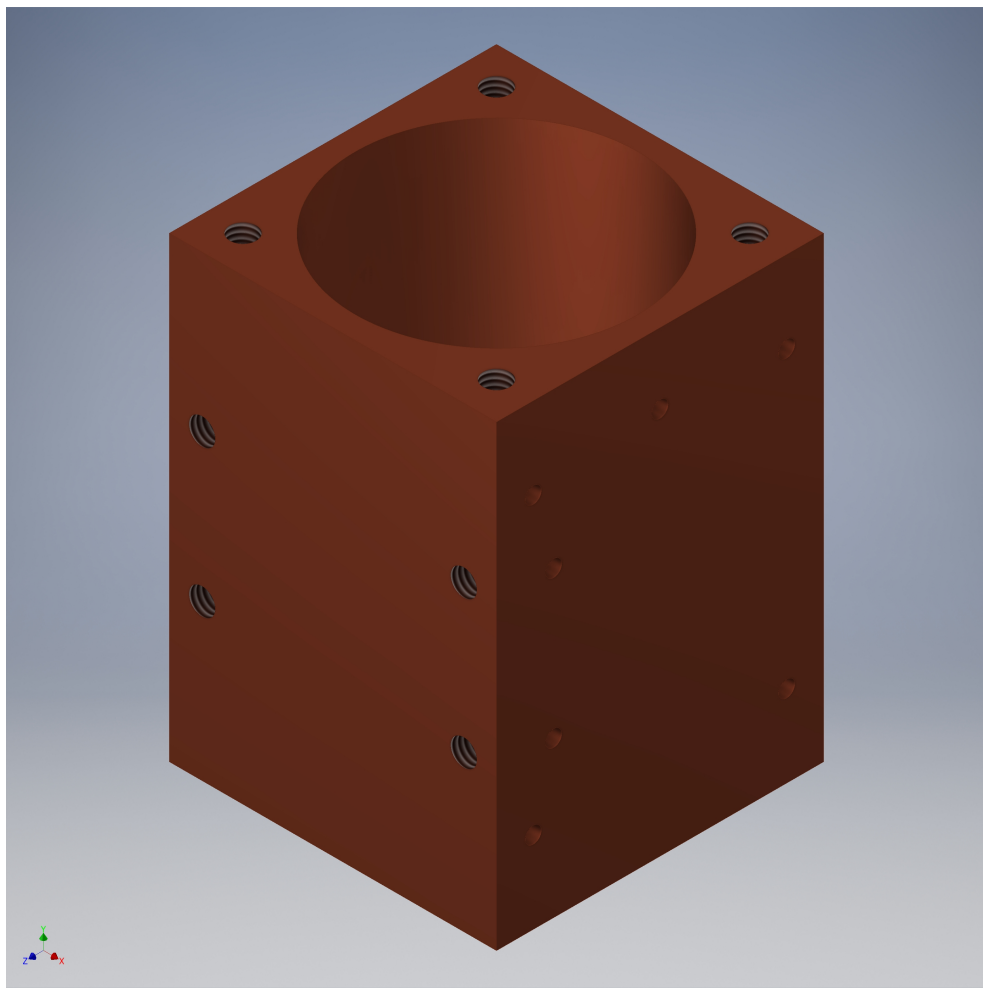


Figure 36: 3D model of a shield

3.2.4 Helix

Helix as displayed in the figure 37 features:

- end soldered to the shield (3.2.3)
- end soldered to a SMA on the bottom cap (3.2.2)

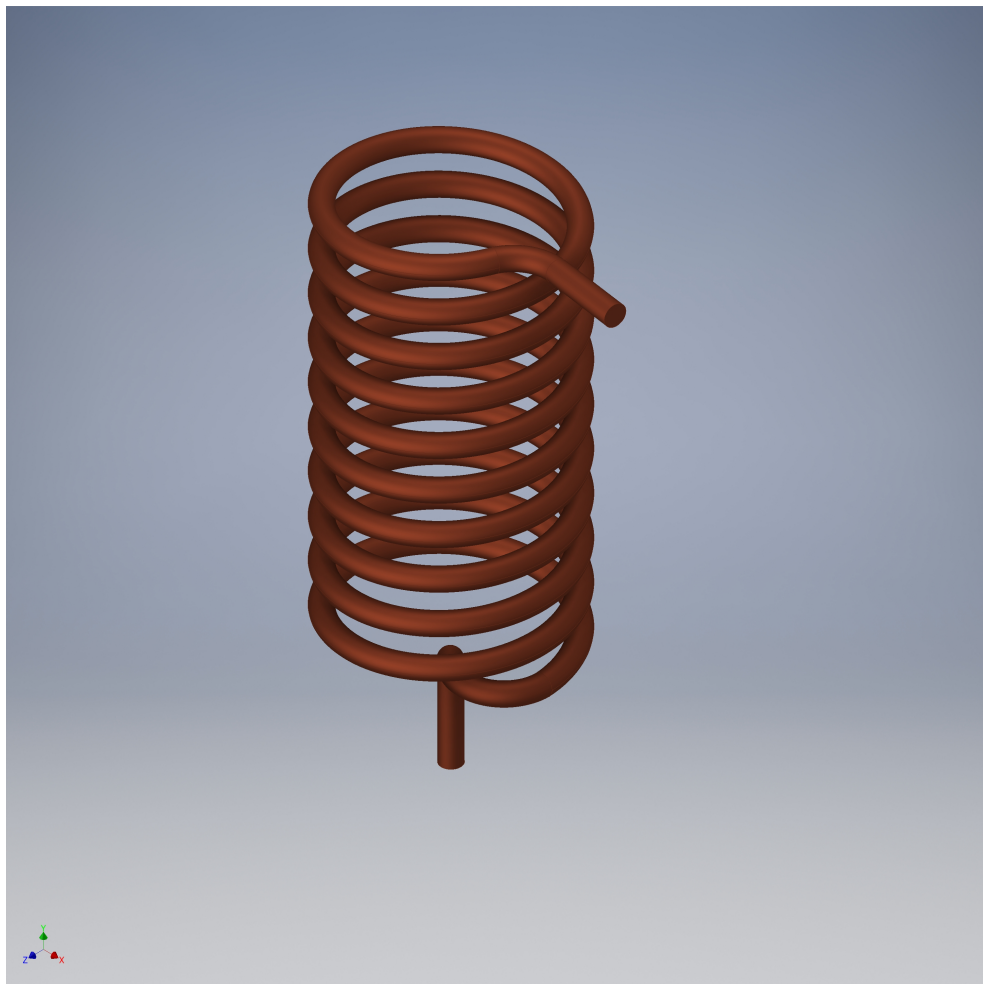


Figure 37: 3D model of a helix

3.2.5 Helix support

Since d_0 as specified in the table 34 is smaller than recommended thickness of 5 mm the question of mechanical stability arises. In order to eliminate potential mechanical oscillations we introduce a helix support made of PEEK to be inserted inside of the helix (3.2.4). PEEK was selected as a cryogenic compatible insulator thus minimizing its influence on the helix's inductivity.

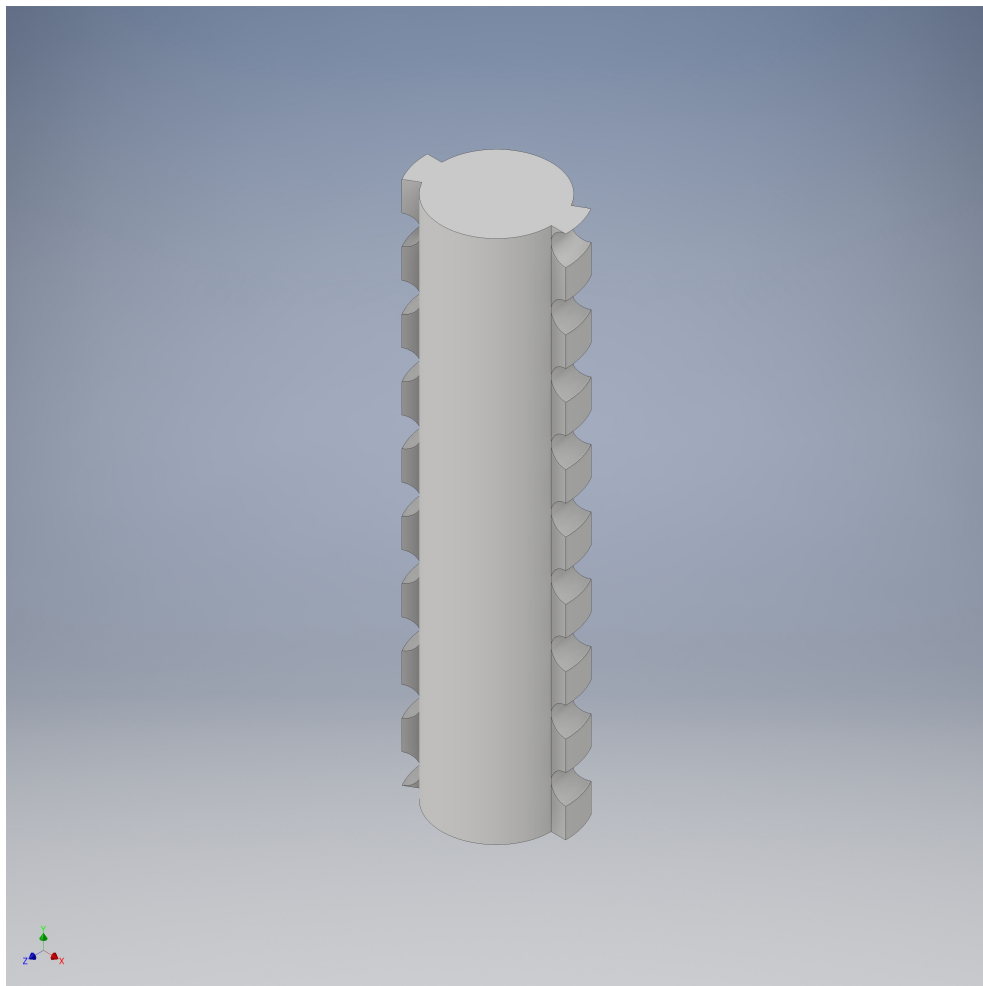


Figure 38: 3D model of a helix support

3.2.6 Top cap

Top cap as displayed in the figure 39 features:

- 4xM4 clearance holes to connect to the shield (3.2.3)
- 4xM2 thread holes to connect to the top cap clamp (3.2.7)
- tight hole for an antenna mount (3.2.8)
- angular scale for an antenna mount (3.2.8)

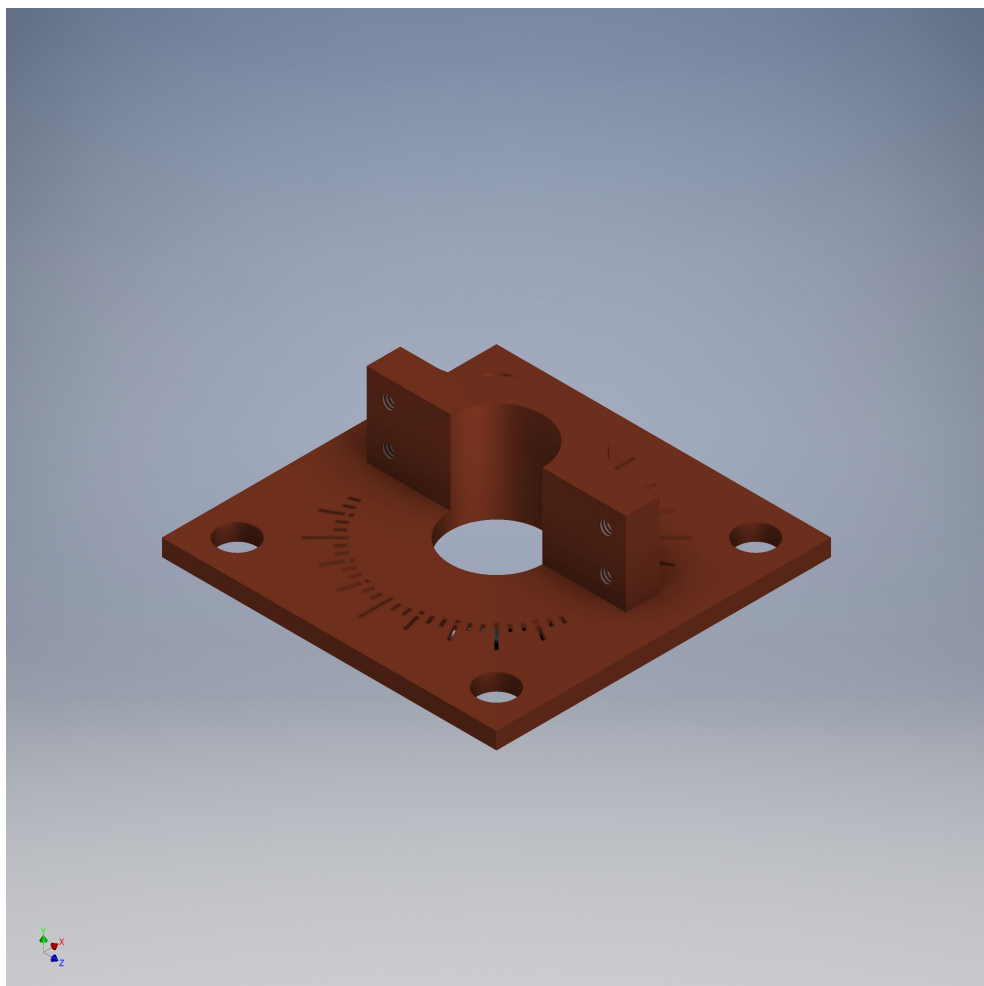


Figure 39: 3D model of a top cap

3.2.7 Top cap clamp

Top cap clamp as displayed in the figure 310 features:

- 4xM2 clearance holes to connect to the top cap (3.2.6)
- truncated semicircle to clamp an antenna mount (3.2.8)

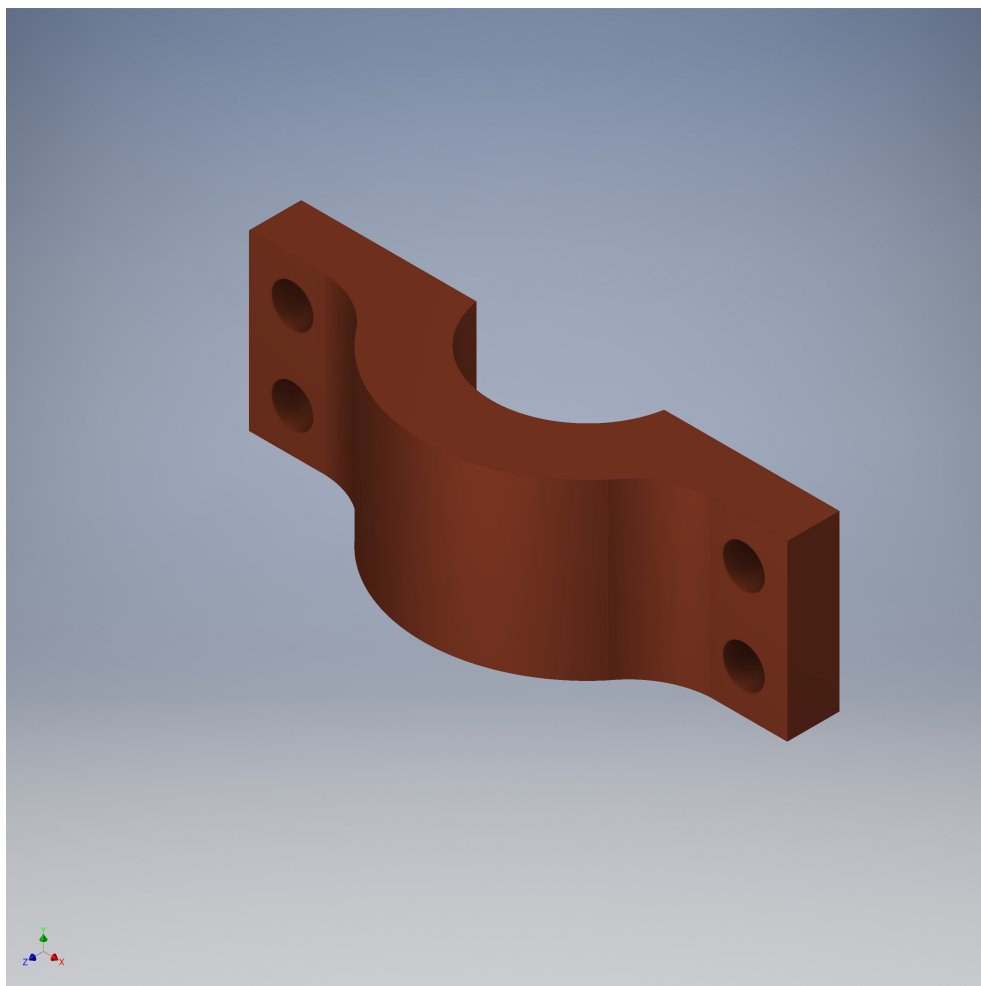


Figure 310: 3D model of a top cap clamp

3.2.8 Antenna mount

Antenna mount as displayed in the figure 311 features:

- 2xM2 thread holes for a SMA connector for the antenna (3.2.9)
- hole for the antenna (3.2.9)
- cut for a precise usage of the angular scale on the top cap (3.2.6)
- 1 mm period cuts to determine the distance to the top cap (3.2.6)

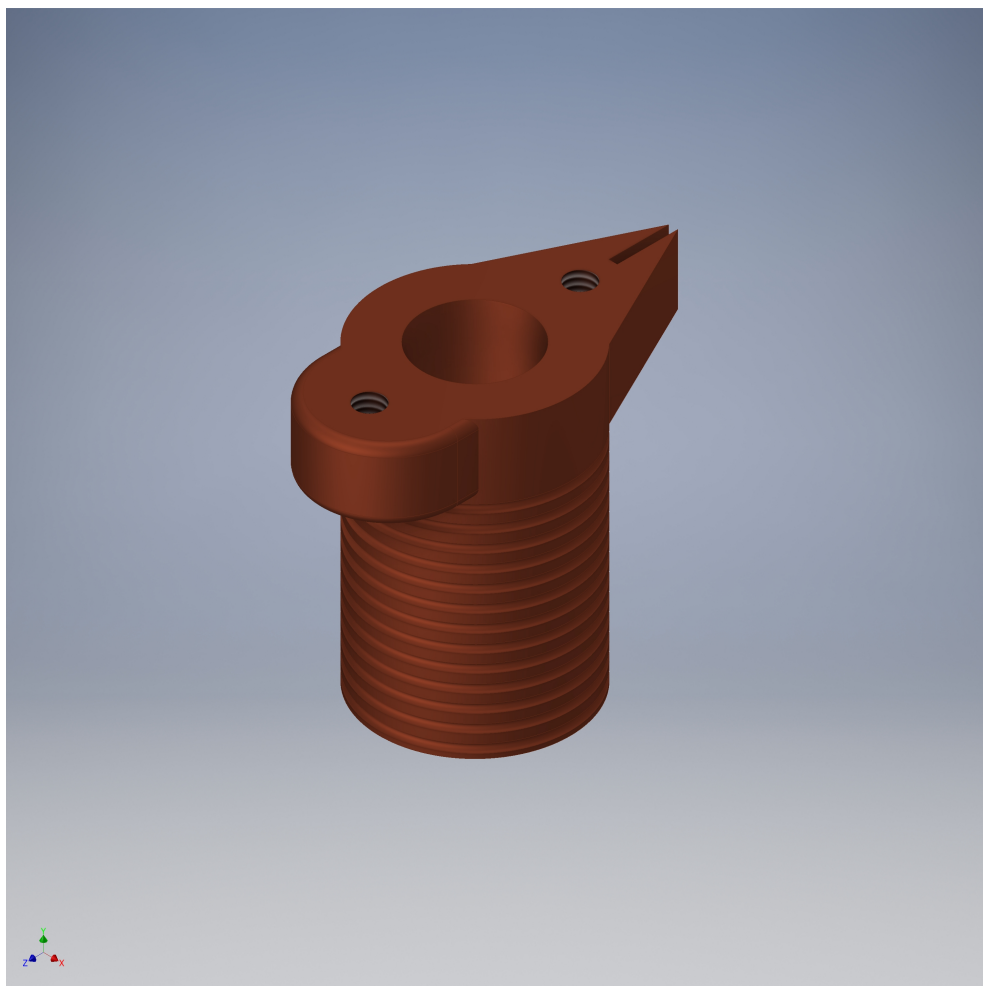


Figure 311: 3D model of an antenna mount

3.2.9 Antenna

Antenna as displayed in the figure 312 features:

- end connecting to a SMA on the antenna mount (3.2.8)
- end soldered to the bottom of the antenna mount (3.2.8)
- using empirical estimation from [17] a diameter of 11 mm was selected

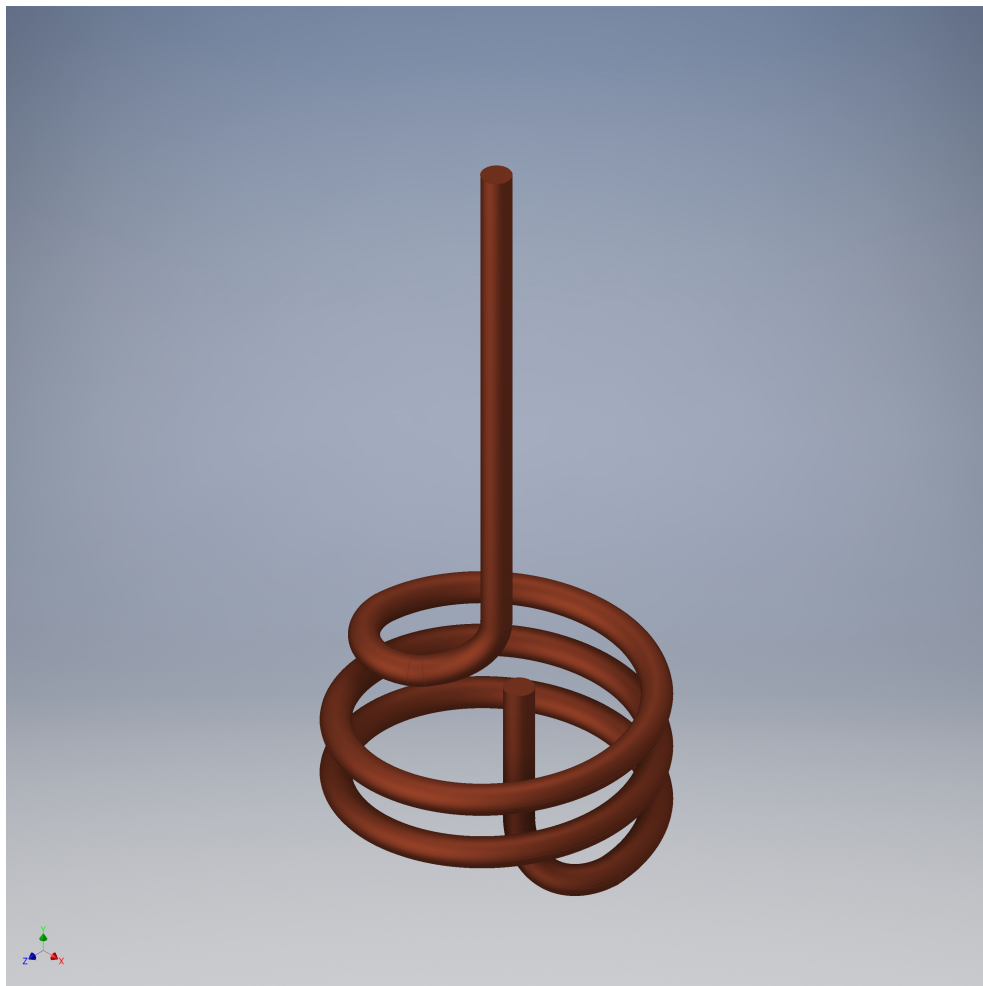


Figure 312: 3D model of an antenna

Chapter 4

Validation

Chapter 5

External circuits & additional features

Appendix A

Mathematica code for Macalpine's model

This is a relevant part of the script supporting calculations in [12].

```
In[1]:= (* Physical Constants and Units *)
μ0 = 4*π*10-7;
ε0 = 8.854187817*10-12;
c = 299792458;
AMU = 1.6605402*10-27;
h = 6.6260755*10-34;
ℏ =  $\frac{h}{2\pi}$ ;
μB = 9.2740154*10-24;
kB = 1.380658*10-23;
grav = 9.8;
a0 = 0.5291772108*10-10;
me = 9.1093826*10-31;
ee = 1.60217733*10-19; eV = ee;
Eh =  $\frac{\hbar^2}{me a_0^2}$ ;
m=1; μm=10-6m; mm=10-3m; cm=10-2m; nm=10-9m; km=103m;
in=2.54cm; ft=12in; mi=5280*ft;
K=1; mK=10-3K; μK=10-6; nK=10-9K; pK=10-12;
T=1; mT=10-3K; G=10-4; mG=10-3G; μG=10-6;
sec=1; s=1; ms=10.0-3s; μs=10-6s; ns=10-9s;
Ω=1; mΩ=10-3; kΩ=103; MΩ=106;
A=1; mA=10-3A; μA=10-6; nA=10-9;
W=1; mW=10-3; μW=10-6; nW=10-9;
Hz=1; kHz=103; MHz=106; GHz=109;
nF=10-9; pF=10-12;
nH=10-9; pH=10-12;
```

```

In[2]:= (* Calculations for Cu resonator *)
Ds[Bs_]:= 0.75Bs; (*diameter of shield*)
d[Bs_]:= 0.55Ds[Bs]; (*diameter of helix*)
b[Bs_]:= 1.5d[Bs]; (*length of helix*)

Nt[Bs_,f0_]:=  $\frac{48.26 \cdot 10^6}{f0 \cdot Ds[Bs]}$ ; (*number of turns*)
d0[Bs_,f0_]:= 0.5  $\frac{b[Bs]}{Nt[Bs, f0]}$ ; (*diameter of wire*)
 $\tau[Bs_, f0_] := \frac{b[Bs]}{Nt[Bs, f0]}$ ; (*pitch*)

(*effective inductance*)
Leff[Bs_,f0_]:=  $9.84 \cdot 10^{-7} \cdot \left( \frac{Nt[Bs, f0] \cdot d[Bs]}{b[Bs]} \right)^2 \cdot \left( 1 - \left( \frac{d[Bs]}{Ds[Bs]} \right)^2 \right)$ ;
Ceoff[Bs_]:=  $\frac{2.95 \cdot 10^{-11}}{\log_{10} \frac{Ds[Bs]}{d[Bs]}}$ ; (*effective capacitance*)

Z0[Bs_,f0_]:=  $\sqrt{\frac{Leff[Bs, f0]}{Ceoff[Bs]}}$ ; (*characteristic impedance*)
v[Bs_,f0_]:=  $\frac{1}{\sqrt{Leff[Bs, f0] \cdot Ceoff[Bs]}}$ ; (*velocity*)
 $\lambda[Bs_, f0_] := \frac{v[Bs, f0]}{f0}$ ; (*wavelength*)

Q[Bs_,f0_]:= 1.97 Ds[Bs]  $\sqrt{f0}$ ;

omega[Bs_,f0_,Cl_]:= Module[{w},
  w =  $v/.FindRoot[\frac{1}{2\pi \cdot Z0[Bs, f0] \cdot Cl \cdot v} == \tan(\frac{2\pi v \cdot b[Bs]}{v[Bs, f0]})]$ , {v, f0}] [[1]];
  Return@w;
]

In[3]:= Bs = 60mm; (*length of shield*)
(* This frequency needs to be varied
until loaded frequency is close to target frequency*)
f0 = 97.023MHz; (*center frequency*)
Cl = 10pF; (*trap capacitance*)

Print["Bs = ", Bs/mm, " mm (length of shield)"]
Print["Ds = ", Ds[Bs]/mm, " mm (diameter of shield)"]
Print["d = ", d[Bs]/mm, " mm (diameter of helix)"]
Print["b = ", b[Bs]/mm, " mm (length of helix)"]
Print["Nt = ", Nt[Bs,f0], " (number of turns)"]
Print["d0 = ", d0[Bs,f0]/mm, " mm (diameter of wire)"]

```

```

Print["τ = ",τ[Bs,f0]/mm," mm (pitch of helix)"]
Print["Z₀ = ",Z₀[Bs,f0]/ω," ω (characteristic impedance)"]
Print["Lᵅᵅᵅ = ",Lᵅᵅᵅ[Bs,f0]/(nH/mm)," nH/mm (effective inductance)"]
Print["Cᵅᵅᵅ = ",Cᵅᵅᵅ[Bs]/(pF/mm)," pF/mm (effective capacitance)"]
Print["v = ",v[Bs,f0]/(m/s)," m/s (velocity)"]
Print["λ = ",λ[Bs,f0]/mm," mm (wavelength)"]
Print["f₀ = ",f₀/MHz," MHz (unloaded frequency)"]
Print["Q = ",Q[Bs,f0]," (quality factor)"]
Print["ν₀ = ",omega[Bs,f0,C1]/MHz," MHz (loaded frequency)"]

Clear[Bs,f0,C1];
Bs = 60 mm (length of shield)
Ds = 45. mm (diameter of shield)
d = 24.75 mm (diameter of helix)
b = 37.125 mm (length of helix)
Nt = 11.0535 (number of turns)
d₀ = 1.67933 mm (diameter of wire)
τ = 3.35866 mm (pitch of helix)
Z₀ = 572.731 Ω (characteristic impedance)
Lᵅᵅᵅ = 37.2698 nH/mm (effective inductance)
Cᵅᵅᵅ = 0.11362 pF/mm (effective capacitance)
v = 1.53672*10^7 m/s (velocity)
λ = 158.387 mm (wavelength)
f₀ = 97.023 MHz (unloaded frequency)
Q = 873.205 (quality factor)
ν₀ = 40. MHz (loaded frequency)

```

Appendix B

Mathematica code for Siversns' model

Following calculations are heavily based on a script generously provided by James David Siversns. All variables and references correspond to [17].

```
In[1]:= (* Units and constants *)
MHz = 106;
pF = 10-12;
Ω = 1;
mm = 10-3;
m = 1;
H = 1;
μ0 = 4π*10-7;

In[2]:= (* Trap and wire values *)
Cw = 0.00001 pF; (* Wire to trap capacitance *)
Rt = 0.1 Ω; (* Trap resistance *)
CΣ[Ct_] := Cw + Ct; (* Sum of above *)

In[3]:= calculateQ[dMillimeters_, γ_]:=Module[{
(* Arguments naming as in Siversns paper *)
d0, τ, d, De, α, ρ, eN, b, Cc, KLC, KCs, Cs, LC, ω0, δ, lc, r, Ns, ls, a,
Rs, Rc, Rj, XLc, XCc, Xct, Xcw, XCs, Zcoil, ZE, Ztot, RealZ, Q,
maxSize, log, ωRes, Capacitance
},
Capacitance = 20pF;
(* Switch log function for plotting *)
log = Print;
log = (#)&

(* Resonator parameters *)
(* Coil wire diameter, we take it from Macalpine *)
d0 = 1.95mm;
```

```

 $\tau = 2*d0$ ; (* Winding pitch *)
 $d = d\text{Millimeters}*\text{mm}$ ; (* Diameter of coil *)
 $De = d/\gamma$ ; (* Diameter of a shield *)
 $\alpha = d/De$ ;
(* Resistivity of resonator material *)
 $\rho = 1.7*10^{-8}*\Omega*\text{m}$ ;
(* Given by the 4K chamber design *)
maxSize = 36mm;
b = 56mm - De/2;
(* Handling case of a too large resonator *)
If[d>maxSize || De>maxSize || b<=0, Return@0];

log["b = ", b/mm, "mm"];
log["d = ", d/mm, "mm"];
log["D = ", De/mm, "mm"];

eN = b/tau; (* Number of turns in the coil *)
log["N = ", eN];
(* Coil self capacitance - equation 25 *)

Cc = ((11.26  $\frac{b}{d}$ ) + 8 + ( $\frac{27}{\sqrt{\frac{b}{d}}}$ ))d pF;

KLC = 39.37  $\frac{0.025 \left(\frac{d}{\tau}\right)^2 (1-\alpha^2)}{\left(\frac{d}{\tau}\right)^2}$  10-6 H/m;
KCs = 39.37  $\frac{0.75}{\text{Log}[10, \frac{1}{\alpha}]}$  pF/m;

(* Shield-coil capacitance - equation 26 *)
Cs = b KCs;
(* Inductance of coil inside a shield - equation 27 *)
LC = b KLC;
(* Resonant frequency - equation 21 *)
ωRes[Ct_] :=  $\frac{1}{\sqrt{(Cs+Ct+Cw+Cc)LC}}$ ;

log["ω = ", ωRes[Capacitance]/(2π MHz), "MHz"];

ω0[Ct_] := 2π*40 MHz; (* This is a target frequency *)
(* Allowing 15% accuracy for the frequency *)
If[
     $\frac{\text{Abs}[\omega_0[\text{Capacitance}] - \omega_{\text{Res}}[\text{Capacitance}]]}{\omega_0[\text{Capacitance}]}$  > 0.15,
    Return@0
];

```

```

δ[Ct_]:= Sqrt[ $\frac{2 \rho}{(\omega_0[\text{Ct}] \mu_0)}$ ]; (* Skin depth *)
(* Unwond length of the coil *)
lc =  $2\pi \sqrt{\left(\frac{d}{2}\right)^2 + \left(\frac{\tau}{2\pi}\right)^2} \frac{b}{\tau}$ ;
r =  $\frac{d}{2} \left(\frac{1}{\alpha} - 1\right)$ ;
(* Number of "turns" in the currents path in the shield
- equation 31 *)
Ns =  $\frac{b \cdot lc}{4\pi r^2}$ ;
(* Distance of current path in the shield - equation 32 *)
ls = Ns Sqrt[ $\pi^2 \left(\frac{d}{\alpha}\right)^2 + \left(\frac{b}{Ns}\right)^2$ ];
a[Ct_]:=  $\frac{Ct}{Cs + Cw}$ ;
Rs[Ct_]:=  $\frac{\rho \cdot ls}{b \delta[\text{Ct}]}$ ;
Rc[Ct_]:=  $\frac{\rho \cdot lc}{d_0 \pi \delta[\text{Ct}]}$ ;
(* Resistance of solder joint as a function of frequency -
the 0.003 is the DC resistance of a typical solder joint
between shield and coil, however this can vary
and is best to measure *)
Rj[Ct_]:= 0.003 Sqrt[ $\frac{\omega_0[\text{Ct}]}{2\pi \cdot 10^5}$ ] Ω;
(* Q calculations *)
XLc[Ct_]:= ω0[Ct] LC;
XCc[Ct_]:=  $\frac{1}{\omega_0[\text{Ct}] Cc}$ ;
Xct[Ct_]:=  $\frac{1}{\omega_0[\text{Ct}] Ct}$ ;
Xcw[Ct_]:=  $\frac{1}{\omega_0[\text{Ct}] Cw}$ ;
XCs[Ct_]:=  $\frac{1}{\omega_0[\text{Ct}] Cs}$ ;
Zcoil[Ct_]:=  $\left( \frac{1}{(i XLc[\text{Ct}] + Rc[\text{Ct}]) + \frac{1}{i XCc[\text{Ct}]}} \right)^{-1}$ ;
ZE[Ct_]:=  $\left( \frac{1}{(\frac{1}{i} Xct[\text{Ct}] + Rj[\text{Ct}]) + \frac{1}{i} Xcw[\text{Ct}] + \frac{1}{i} XCs[\text{Ct}]} \right)^{-1}$ ;

```

```

Ztot[Ct_] := Zcoil[Ct] + ZE[Ct] + Rs[Ct] + Rj[Ct];

RealZ[Ct_] := 
$$\frac{Rc[Ct] \cdot XCc[Ct]^2}{Rc[Ct]^2 + (XCc[Ct] - XLc[Ct])^2} +$$


$$\frac{Rt \cdot XCs[Ct]^2 \cdot Xcw[Ct]^2}{Rt^2(XCs[Ct] + Xcw[Ct])^2 + (XCs[Ct](Xct[Ct] + Xcw[Ct]) + Xct[Ct]Xcw[Ct])^2}$$

+ Rs[Ct] + Rj[Ct];

Q[Ct_] := 
$$\frac{LC \cdot \omega_0[Ct]}{RealZ[Ct]}$$
;

Return@Q[Capacitance];
]

In[4]:= SetDirectory[NotebookDirectory[]];
contourData = Table[
{γ, d, calculateQ[d, γ]},
{d, 15, 25, 0.01},
{γ, 0.4, 0.7, 0.01}
] // Flatten[#, 1]&;

ListContourPlot[
contourData,
PlotLegends → Automatic,
FrameLabel → {"d/D", "d, mm"}
]

In[5]:= (* Final parameters *)
calculateQ[19, 0.55]

b = 38.7273mm
d = 19mm
D = 34.5455mm
N = 9.93007
ω = 39.7919MHz

Out[5]= 362.188

```

Bibliography

- [1] K. Deng, Y. L. Sun, W. H. Yuan, Z. T. Xu, J. Zhang, Z. H. Lu, and J. Luo. A modified model of helical resonator with predictable loaded resonant frequency and Q-factor. *Review of Scientific Instruments*, 85(10):1–8, 2014.
- [2] Paul A. M. Dirac. On the Theory of Quantum Mechanics. *Proceedings of the Royal Society A: Mathematical, Physical and Engineering Sciences*, 112(762):661–677, oct 1926.
- [3] Richard Phillips Feynman. The Wonders That Await a Micro-Microscope. *The Saturday Review*, pages 45–47, 1960.
- [4] Davide Gandolfi. *Compact RF Amplifier for Scalable Ion-Traps*. PhD thesis, Università degli Studi di Trento and Universität Innsbruck, 2010.
- [5] Amy Greene. *Experiments Towards Mitigation of Motional Heating in Trapped Ion Quantum Information Processing*. Master of engineering in electrical engineering and computer science thesis, Massachusetts Institute of Technology, 2016.
- [6] S. Gulde. *Experimental realization of quantum gates and the Deutsch-Josza algorithm with trapped ^{40}Ca -ions*. PhD thesis, University of Innsbruck, 2017.
- [7] K G Johnson, J. D. Wong-Campos, A Restelli, K A Landsman, B Neyenhuis, J Mizrahi, and C. Monroe. Active stabilization of ion trap radiofrequency potentials. *Review of Scientific Instruments*, 87(5):053110, may 2016.
- [8] T. Karin, I. Le Bras, A. Kehlberger, K. Singer, N. Daniilidis, and H. Häffner. Transport of charged particles by adjusting rf voltage amplitudes. *Applied Physics B*, 106(1):117–125, jan 2012.

Bibliography

- [9] Ezra Kassa, Hiroki Takahashi, Costas Christoforou, and Matthias Keller. Precise positioning of an ion in an integrated Paul trap-cavity system using radiofrequency signals. *Journal of Modern Optics*, 65(5-6):520–528, mar 2018.
- [10] Ezra M. B. Kassa. *Single ion coupled to a high-finesse optical fibre cavity for cQED in the strong coupling regime*. Doctor of philosophy thesis, University of Sussex, 2016.
- [11] Muir Kumph. *2D Arrays of Ion Traps for Large Scale Integration of Quantum Information Processors*. PhD thesis, University of Innsbruck, 2015.
- [12] Florian Michael Leupold. *Bang-bang Control of a Trapped-Ion Oscillator*. PhD thesis, ETH Zurich, 2015.
- [13] W. Macalpine and R. Schildknecht. Coaxial Resonators with Helical Inner Conductor. *Proceedings of the IRE*, 47(12):2099–2105, dec 1959.
- [14] Wolfgang Paul. Electromagnetic Traps for Charged and Neutral Particles(Nobel Lecture). *Angewandte Chemie International Edition in English*, 29(7):739–748, jul 1990.
- [15] A.M. Prokhorov. Joule–Lenz law. *Great Soviet Encyclopedia*, 1972.
- [16] Felix Rohde. *Remote ion traps for quantum networking: Two-photon interference and correlations*. Dissertation, ICFO Barcelona, 2009.
- [17] J. D. Siverns, L. R. Simkins, S. Weidt, and W. K. Hensinger. On the application of radio frequency voltages to ion traps via helical resonators. *Applied Physics B*, 107(4):921–934, jun 2012.
- [18] Q. A. Turchette, Kielpinski, B. E. King, D. Leibfried, D. M. Meekhof, C. J. Myatt, M. A. Rowe, C. A. Sackett, C. S. Wood, W. M. Itano, C. Monroe, and D. J. Wineland. Heating of trapped ions from the quantum ground state. *Physical Review A*, 61(6):063418, may 2000.
- [19] Andre J. S. Van Rynbach. *Microfabricated Surface Trap and Cavity Integration for Trapped Ion Quantum Computing by Abstract Microfabricated Surface Trap and Cavity Integration for Trapped Ion Quantum Computing*. Doctor of philosophy dissertation, Graduate School of Duke University, 2016.

Declaration of originality

The signed declaration of originality is a component of every semester paper, Bachelor's thesis, Master's thesis and any other degree paper undertaken during the course of studies, including the respective electronic versions.

Lecturers may also require a declaration of originality for other written papers compiled for their courses.

I hereby confirm that I am the sole author of the written work here enclosed and that I have compiled it in my own words. Parts excepted are corrections of form and content by the supervisor.

Title of work (in block letters):

Authored by (in block letters):

For papers written by groups the names of all authors are required.

Name(s):

First name(s):

With my signature I confirm that

- I have committed none of the forms of plagiarism described in the '[Citation etiquette](#)' information sheet.
- I have documented all methods, data and processes truthfully.
- I have not manipulated any data.
- I have mentioned all persons who were significant facilitators of the work.

I am aware that the work may be screened electronically for plagiarism.

Place, date

Signature(s)

For papers written by groups the names of all authors are required. Their signatures collectively guarantee the entire content of the written paper.